Chitosan/Clay Nanocomposite Film Preparation and Characterization

Yixiang Xu,[1] Xi Ren,[2] Milford A. Hanna[1]

[1]*Industrial Agricultural Products Center and Department of Food Science & Technology, University of Nebraska, Lincoln, Nebraska 68583-0730*
[2]*Department of Engineering Mechanics, University of Nebraska, Lincoln, Nebraska 68588-0526*

Received 06 January 2005; accepted 19 May 2005
DOI 10.1002/app.22664
Published online in Wiley InterScience (www.interscience.wiley.com).

ABSTRACT: Nanocomposites of chitosan and nanoclays (MMT-Na^+ and Cloisite 30B) were prepared by solvent casting. The structural properties, thermal behaviors, and mechanical properties were characterized using X-ray diffraction (XRD), transmission electron microscopy (TEM), atomic force microscopy, differential scanning calorimetry, thermogravimetry analyses, and an Instron universal testing machine. XRD and TEM results indicated that an exfoliated structure was formed with addition of small amounts of MMT-Na^+ to the chitosan matrix. Intercalation along with some exfoliation occurred with up to 5 wt % MMT-Na^+. Micro-scale composite (tactoids) formed when Cloisite 30B was added to the chitosan matrix. Surface roughness increased with addition of a small amount of clay. Tensile strength of a chitosan film was enhanced and elongation-at-break decreased with addition of clay into the chitosan matrix. Melt behavior and thermal stability did not change significantly with addition of clays. © 2005 Wiley Periodicals, Inc. J Appl Polym Sci 99: 1684–1691, 2006

Key words: chitosan; nanocomposites; structure; mechanical properties; thermal properties

INTRODUCTION

Chitosan derived from chitin, an abundant polysaccharide found in shellfish, possesses a unique cationic nature relative to other neutral or negatively charged polysaccharides. The amino group, NH_2, in chitosan can be protonated to NH_3^+ in an acid environment, resulting in antifungal or antimicrobial activities, since cations can bind with anionic sites in protein.[1] Further, chitosan is a nontoxic natural polysaccharide and is compatible with living tissue. These distinguishing features make chitosan widely applicable in healing, artificial skin, food preservation, cosmetics, and wastewater treatment.[2–7] However, chitosan's hydrophilic character, and consequently its poor mechanical properties in the presence of water and humid environments, limits its application.

Developing chitosan-layered silicate nanocomposites by inserting chitosan chains into interlayers of silicate can improve its mechanical properties. In recent years, polymer nanocomposites have received considerable interest because of their superior thermal and mechanical properties, as compared with the polymer itself.[8] Polymer-clay nanocomposites are a class of hybrid materials composed of organic polymer matrices and nanoscale organophilic clay fillers.[9] Of the nanoscale clays, montmorillonite (MMT) is of particular interest and has been studied widely. MMT is a hydrated alumina-silicate layered clay made up of two silica tetrahedral sheets fused to an edge-shared octahedral sheet of aluminum hydroxide. Its advantages of high surface area, large aspect ratio (50–1000), and platelet thickness of 10 Å make it suitable for reinforcement purposes.[10] The inorganic surface of MMT has also been modified by organic replacement of the interlayer sodium ions by various organic cations to make the platelets more compatible with polymers.[11]

When nanoclay is mixed with a polymer, three types of composites (tactoids, intercalation, and exfoliation) can be obtained (Fig. 1). In the case of tactoids, complete clay particles are dispersed within the polymer matrix and the layers do not separate. Mixing a polymer and organoclay forms a micro-scale composite, with the clay serving only as a conventional filler. Intercalation and exfoliation are two ideal nano-scale composites. Intercalation occurs when a small amount of polymer is inserted between the layers of the clay, thus expanding the interlayer spacing and forming a well-ordered multilayer structure. In exfoliation, the layers of the clay are separated completely and the individual layers are distributed throughout the polymer matrix.[12] The formation of intercalation or exfoliation depends on the types and amounts of nanoclay used.

Correspondence to: M. A. Hanna (mhannal@unl.edu).

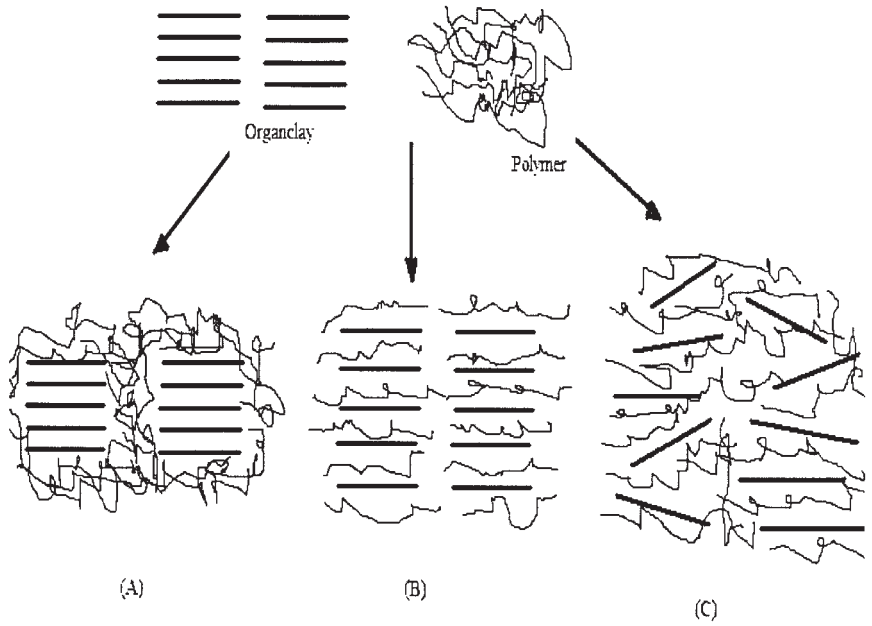

Figure 1 Schematic of possible composite structures obtained when mixing polymer with Organoclays: (A) tactoids, (B) intercalation, and (C) exfoliation.[11]

Yamaguchi et al.[13] prepared a chitosan/hydroxyapatite nanocomposite for orthopedic use. No other reports are available in the open literature. Therefore, the objective of this study was to prepare chitosan/clay nanocomposites using solution intercalation, and then to investigate the nanostructure and functional properties of the chitosan/nanoclay hybrids.

EXPERIMENTAL

Materials

Chitosan powder, with a deacetylation degree of 90%, was purchased from Vanson (Redmond, WA). Two nanoclays, under the trade names of Cloisite Na^+ and Cloisite 30B, were purchased from Southern Clay Co. (Gonzales, TX). Cloisite Na^+ is a natural sodium MMT, while Cloisite 30B is an organically modified sodium in MMT, with a quaternary ammonium salt (methyl-tallow-bis-2-hydroxyethyl ammonium). The particle size range of the nanoclays was 2–13 μ.

Nanocomposite film preparation

A chitosan aqueous solution of 2 wt % was prepared by dissolving 20 g of chitosan powder in 1000 mL of acetic acid solution (1%, v/v). After the chitosan was dissolved, the solutions were filtered with cheesecloth by vacuum aspiration to remove foam and any undissolved impurity.

Nanoclay solutions with three clay compositions (1 wt %, 3 wt %, and 5 wt % based on chitosan) were prepared by dispersing appropriate amounts of clays into 10 mL of 1% acetic acid solution and vigorously stirring for 24 h. Afterwards, 200 mL of chitosan solution was added slowly into pretreated clay solutions. The mixtures were stirred continuously for 4 h and then cast onto level Teflon-coated glass plates. After drying at room temperature for at least 72 h, the films were peeled from the plates.

X-ray diffraction (XRD)

The x-ray patterns of the samples were obtained using a Rigaku D/Max- B X-ray diffractometer (Tokyo, Japan), with Cu-Kα radiation (λ = 1.544 Å) at a voltage of 40 kV and 30 mA. Samples were scanned over the range of diffraction angle 2θ = 1–12°, with a scan speed of 1°/min at room temperature.

Transmission electron microscopy (TEM)

TEM was used to evaluate the dispersion of nanoclay in the chitosan matrix. The image was obtained on a H7500 TEM (Hitachi Co.) at an accelerating voltage of 80 kV. Ultrathin sections were microtomed at room temperature.

Atomic force microscopy (AFM)

AFM topographic images were obtained using an Autoprobe CP (Park Scientific Instruments) in contact mode and commercial Si_3N_4 tips at ambient pressure and room temperature.

Differential scanning calorimetry (DSC)

DSC measurements were performed with a Perkin–Elmer DSC1 (Norwalk, CT). About 10 mg of the dried, ground samples (<2% moisture) were placed in stainless steel DSC pans (Perkin–Elmer). The samples were heated from 50 to 200°C at a heating rate of 10°C/min in a nitrogen atmosphere. The glass transition temperature (T_g) was taken as the inflection point on the DSC thermograph.

Thermal stability analysis

Thermogravimetric analyses (TGA) were completed with a Perkin–Elmer TGA 7 (Norwalk, CT). Samples were placed in the balance system and heated from 50°C to 650°C at a heating rate of 20°C/min in a nitrogen atmosphere. The onset temperature was calculated using TGA7 software.

Tensile strength (TS) and elongation at-break (E)

TS and E were measured with an Instron Universal Testing Machine (Model 5566, Instron Corp., Canton, MA) following the guidelines of ASTM Standard Method D 882–91.[14] The initial grip separation was set at 50 mm and the crosshead speed was set at 200 mm/min. TS was expressed in MPa and calculated by dividing the maximum load (N) by the initial cross-sectional area (m^2) of the specimen. E was calculated as the ratio of the final length at the point of sample rupture to the initial length of a specimen (50 mm) and expressed as a percentage. TS and E tests were replicated five times for each type of film.

Statistical analyses

The tension strength and elongation-at-break data were analyzed by the general linear models (GLM) in SAS analysis program (SAS Institute Inc., Cary, NC). Duncan's multiple range tests were conducted to check for significant ($P < 0.05$) differences between treatment groups.

RESULTS AND DISCUSSION

Structural properties of chitosan/nanoclay composites

Wide-angle X-ray diffraction (WAXD) is a classical method for determining the gallery height (d-spacing distance) in clay particles.[15] The d-spacing can be determined by the diffraction peak in the XRD patterns, and can be expressed by Bragg's equation ($\lambda = 2d_{001}\sin\theta$), where d_{001} is the interplanar distance of (001) diffraction face, θ is the diffraction position, and λ is the wavelength.[16] During intercalation, the insertion of polymer into the organoclay galleries forces the platelets apart and increases the d-spacing, resulting in a shift of the diffraction peak to lower angles.

The XRD patterns of the chitosan, the two clays, and their composites are shown in Figure 2. The structures of the hybrids depended on the clays used. MMT-Na^+ had a characteristic peak at $2\theta = 7.22°$ ($d_{001} = 12.2$ Å). With addition of 1 and 3 wt % MMT-Na^+ to chitosan solution, the reflection peak disappeared, indicating formation of an exfoliated structure, which was disordered and not detectable by XRD. Further increasing the amount of MMT-Na^+ to 5 wt % gave a broad peak at $2\theta = 5.34°$. This was much lower than that of pristine MMT-Na^+, suggesting the occurrence of intercalation together with some exfoliation. In contrast to MMT-Na^+, Cloisite 30B had a lower diffraction peak at $2\theta = 4.8°$ ($d_{001} = 18.5$ Å) due to replacement of sodium ions with long-chain of quaternary ammonium cations. When Cloisite 30B was added to the chitosan solution, irrespective of amount, the peaks remained at the same position ($2\theta = 4.8°$), indicating that no intercalation had occurred, and that microscale composite-tactoids were formed. The formation of different composites with addition of the different clays to chitosan was attributed to the differences in chemical structures and compatibilities with chitosan. Inorganic and hydrophilic MMT-Na^+ was dispersed easily in the chitosan solution to form a favorable interaction with hydrophilic chitosan. Chitosan chains were intercalated into the silicate layers and the coherent order of MMT-Na^+ was destroyed completely. However, for Cloisite 30B, after organically modifying the sodium in MMT with a quaternary ammonium salt, the clay became organic and its hydrophobicity increased. It was very difficult to disperse Cloisite 30B in the chitosan aqueous solution and to form an intermolecular reaction between clay and chitosan in spite of the presence of the hydroxyl group in the gallery of Cloisite 30 B. Strong polar interactions, especially hydrogen bonding, critically affected the formation of intercalation and exfoliated hybrids.[17]

A TEM micrograph of chitosan nanocomposite with 3 wt % MMT-Na^+ is presented in Figure 3. Good and random dispersion of clay in chitosan matrix was observed. The dark sheets of clay were discrete monolayers in the chitosan matrix. No obvious association between silicate sheets was found. This is consistent with the results of the XRD having an exfoliation structure when 3 wt % MMT-Na^+ was added to chitosan matrix.

The topographic images of the surface for pure chitosan film and chitosan nanocomposite films containing 3 wt % and 5 wt % MMT-Na^+ were determined by AFM and are shown in Figure 4. When 3 wt % MMT-Na^+ was added to the chitosan matrix, the nanocomposite had a rough surface morphology. As the clay content was increased to 5 wt %, a relatively smooth surface was observed. The surface roughness of nano-

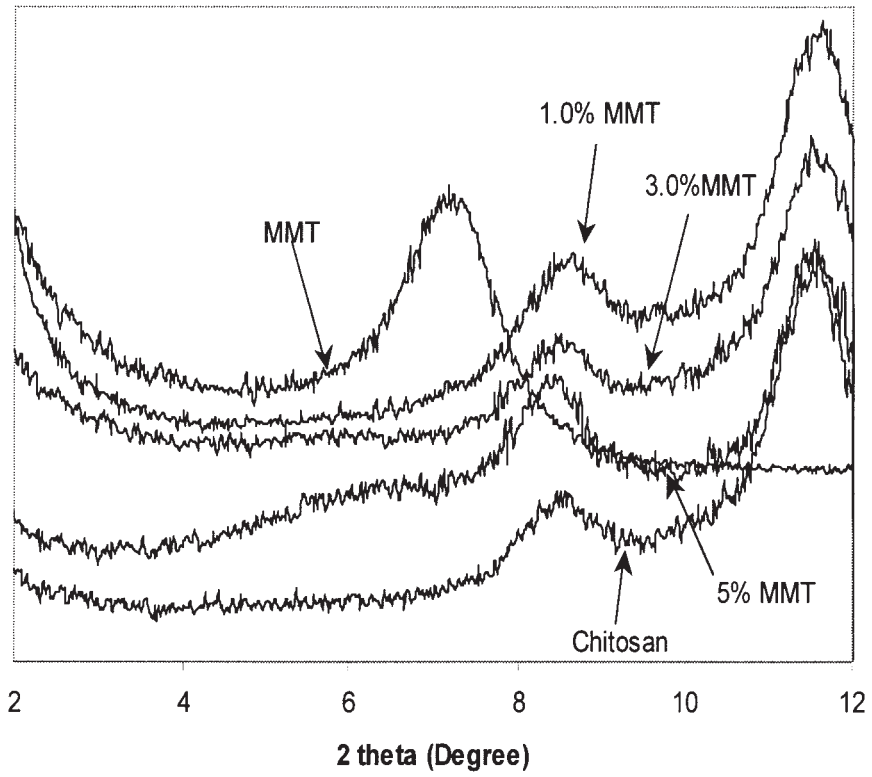

(A)

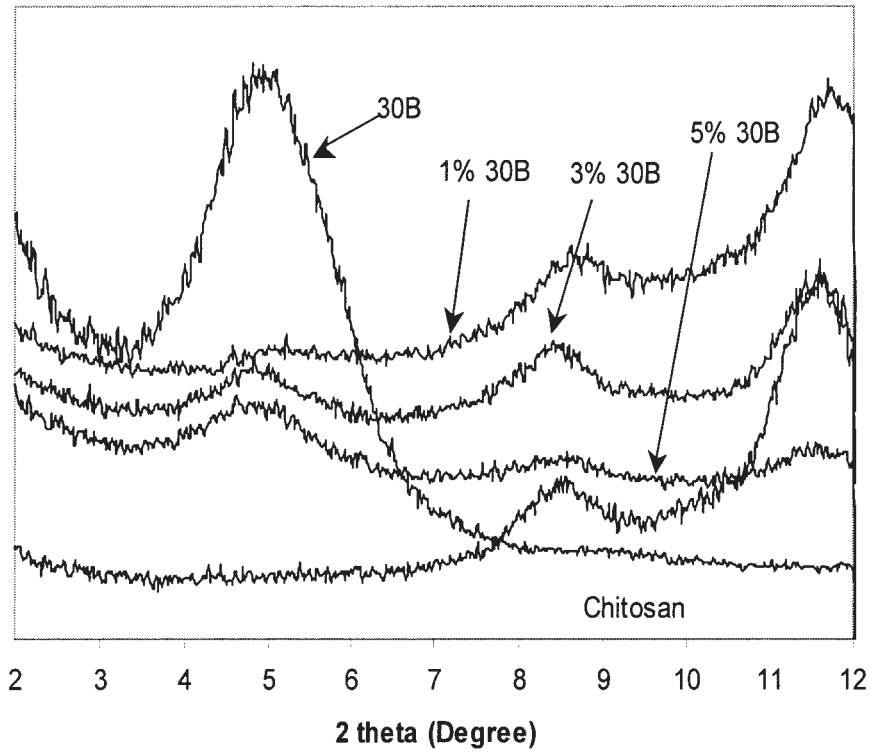

(B)

Figure 2 X-ray patterns of (A) chitosan and its nanocomposites with different amounts of MMT-Na^+ and (B) chitosan and its composites with different amounts of Cloisite 30B.

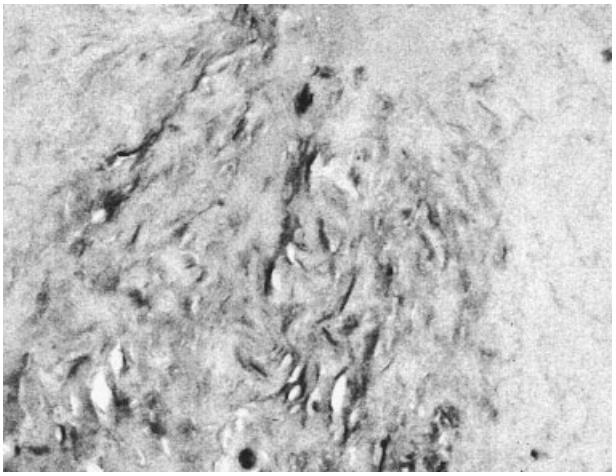

Figure 3 TEM micrographs of chitosan and 3 wt % MMT-Na^+ nanocomposite film.

composite film seemed to decrease with increasing clay content. This was attributed to the fact that the clay had a small particle size and could tumble into the cavities (open cells) on the surface.[18]

Mechanical properties of chitosan/nanoclay composites

The mechanical properties of chitosan and chitosan/clays composite films were measured and are summarized in Table I. The pure chitosan film had a TS of 40.6 MPa and an E of 13.2%. The TS of nanocomposite films increased significantly ($P < 0.05$) with increasing amount of MMT-Na^+ up to 3 wt %, followed by a decrease with further increase in MMT-Na^+ up to 5 wt %. When 1 wt % MMT-Na^+ was added, the TS of the nanocomposite film was 55.0 MPa, an approximately 35% increase compared with that of pure chitosan film. TS was the highest for 3 wt % clay hybrid, in which a 62% improvement was observed. Further increasing clay content to 5 wt % decreased TS of the film to 44.5 MPa. E of the composite film decreased slightly with addition of MMT-Na^+. The substantial enhancement of TS with the addition of a small amount of MMT-Na^+ was ascribed to formation of an exfoliated state and the uniform dispersion of MMT in the chitosan matrix.[19,20] It was also attributed to strong interaction between chitosan and MMT.[16] The decrease in TS with increasing MMT content up to 5 wt % resulted from the aggregation of MMT particles with high surface energy when the MMT content was high enough.[19] This was consistent with XRD patterns having a state where exfoliation coexisted with intercalation. When Cloisite 30B was added to the chitosan matrix, TS did not increase significantly. E decreased significantly when the Cloisite 30B content was increased from 1 to 3 wt %. As discussed previously, a micro-scale composite was formed and the Cloisite 30B clay acted as a conventional filler. Although the filler improved load bearing capacity of the composites, the extent was much lower than that of a nanoscale dispersion.

Thermal properties of chitosan/nanoclay composites

The melting point (T_m) of chitosan and its nanocomposites was investigated by DSC. DSC plots of chitosan and its MMT-Na^+ nanocomposites are presented in Figure 5. The data for all measurements are given in Table II. Two endothermal peaks were detected for all products. The endothermal peak at about 102°C was attributed to solvent evaporation, while the peaks in the range of 188–196°C showed that crystallization of the chitosan was not inhibited by the nanoclays. Pure chitosan film had a T_m of 193.6°C and a melting enthalpy (ΔH_m) of 6.05 J/g. Addition of 1 and 3 wt % MMT-Na^+ increased T_m to 196°C and ΔH_m to 11 J/g, respectively. T_m of the composite film decreased back to 194.5°C when the amount of MMT-Na^+ was increased to 5 wt %. Generally, the changes in T_m, with addition of MMT-Na^+, were not significant, indicating that the crystal forms and the crystal structure of chitosan were not changed.[15] To the contrary, T_m and ΔH_m decreased with the addition of Cloisite 30B. For example, T_m and ΔH_m decreased to 188°C and 3.62 J/g, respectively, with the addition of 5 wt %, suggesting that the degree of crystallinity of chitosan was reduced. These effects can be explained by the assumption that the dispersed Cloisite 30B acted as a physical barrier to hinder the growth of crystals and their perfect ordering.[21]

TABLE I
Mechanical Properties of Chitosan/Nanoclay Composites

Materials	Tensile strengh (MPa)	Elongation at break (%)	Materials	Tensile strength (MPa)	Elongation at break (%)
Chitosan	40.62 ± 0.84^c	13.14 ± 3.85^a	Chitosan	40.62 ± 0.84^a	13.14 ± 3.85^a
1% MMT	54.98 ± 4.83^b	8.72 ± 0.97^a	1% 30B	45.01 ± 0.18^a	14.40 ± 1.47^a
3% MMT	65.67 ± 2.20^a	10.81 ± 0.52^a	3% 30B	47.97 ± 4.91^a	5.71 ± 1.72^b
5% MMT	44.51 ± 3.91^c	8.98 ± 1.21^a	5% 30B	47.29 ± 3.10^a	4.42 ± 0.19^b

[a–c] Means with same letter within a column indicate no significant ($P > 0.05$) difference by Ducan multiple rage test.

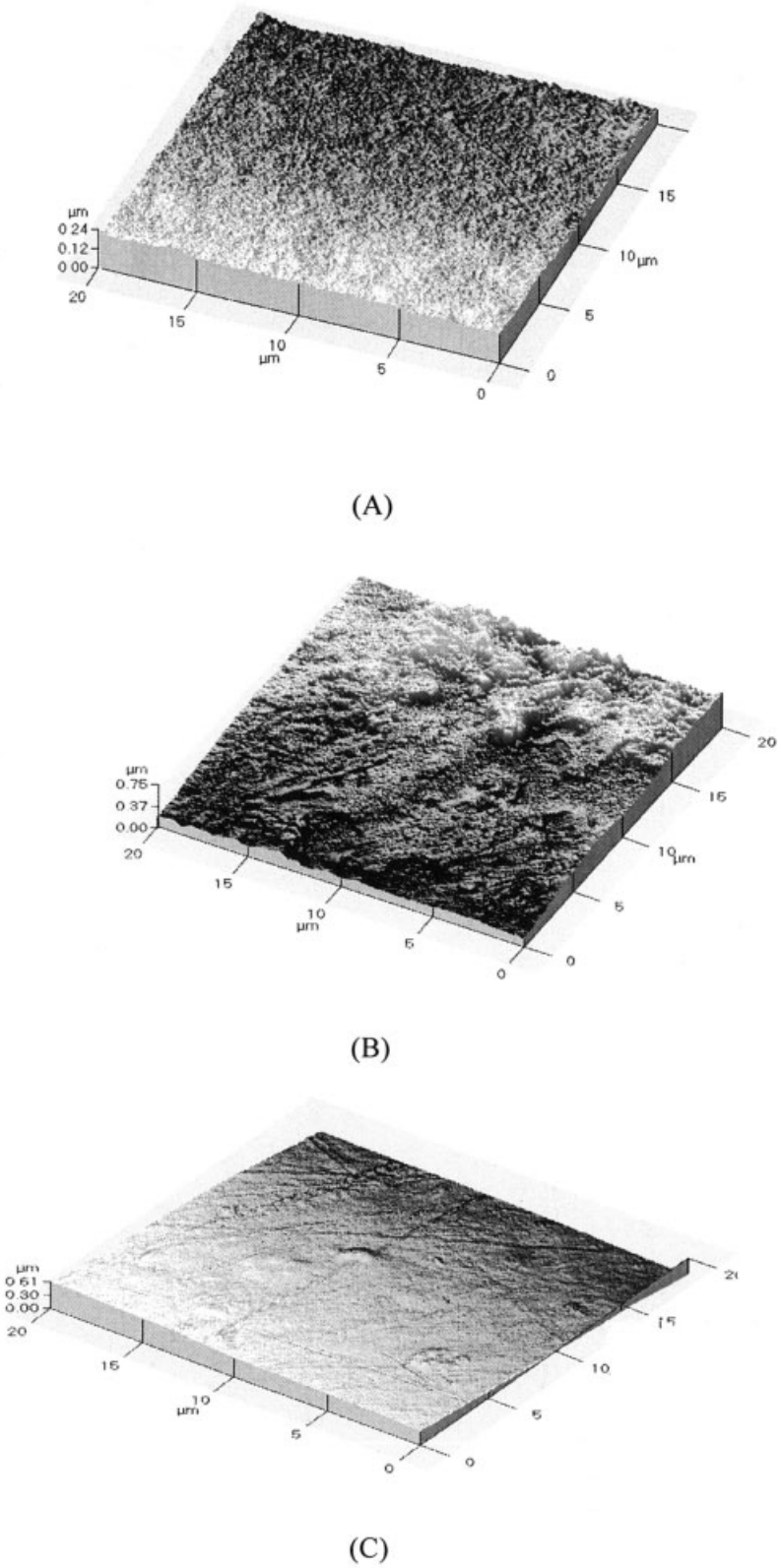

Figure 4 AFM topographic images of (A) chitosan and its nanocomposite films with (B) 3 wt % MMT-Na^+ and (C) 5 wt % MMT-Na^+.

Changes in the thermal stability of chitosan films, with addition of different nanoclays, were examined by TGA and are summarized in Table II. The weight-loss curves of chitosan and its MMT-Na^+ nanocomposites, as a function of temperature, are shown in Figure 6. Generally, the thermal stabilities

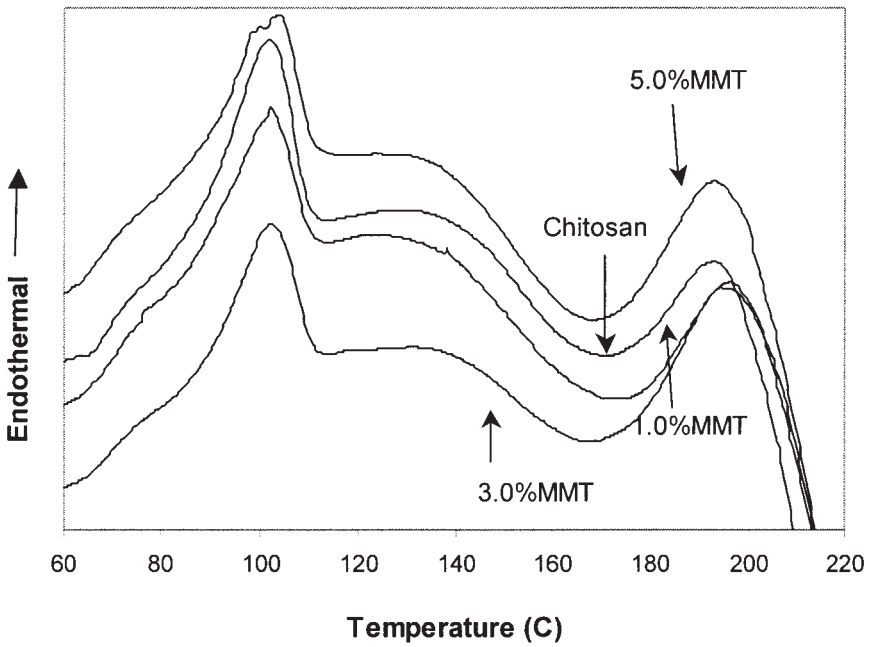

Figure 5 DSC thermographs of chitosan and its MMT-Na^+ nanocomposites with different MMT-Na^+ contents.

of chitosan MMT-Na^+ nanocomposites were enhanced as compared with those of pristine chitosan film. This was reflected by the fact that onset temperatures of thermal degradation increased by 12°C and 7°C, with the incorporation of 1 and 3 wt % MMT-Na^+ into the chitosan. The increase in thermal stability of the nanocomposites was a result of the formation of a nanoscale-composite, in which the chitosan chain penetrated into the galleries of the clay.[21] The nanodispersion of chitosan molecules in the silicate layers not only effectively inhibited the permeation of oxygen, but also restricted their thermal motion, thus increasing thermal stability.[9,16] On the other hand, the onset degradation temperature of chitosan films did not increase significantly with addition of Cloisite 30B. As discussed previously, when Cloisite 30B was added to chitosan, micro-scale composite-tactoids were formed. The polymer chains were not intercalated into the galleries of the silicate and hardly increased the thermal stability. This is consistent with the results of Priya and Jog.[22]

CONCLUSIONS

Exfoliated nano-structures were formed with the addition of small amounts of MMT-Na^+ to the chitosan matrix. Intercalation, together with some exfoliation, occurred with the amounts of MMT-Na^+ increasing to 5 wt %. The surface roughness increased with the addition of a small amount of nanoclay. Micro-scale composite (tactoids) were formed when Cloisite 30B was added to the chitosan matrix. Tensile strength of the chitosan film increased with the addition of small amounts of MMT-Na^+, but not significantly when Cloisite 30B was added. Elongation-at-break decreased with the addition of clays, but not significantly with addition of MMT-Na^+. Melting temperature (T_m) and onset temperature of thermal degradation (T_d) of chitosan composite films increased when MMT-Na^+

TABLE II
Thermal Properties of Chitosan/Nanoclay Composites

Composition	$Peak_1$ (°C)	T_m (°C)	ΔH_m (J/g)	Initial degradation temperature (°C)
Chitosan	102.2	193.6	6.05	294.2
Chitosan + 1% MMT	102.1	196.8	11.37	306.1
Chitosan + 3% MMT	102.1	196.7	11.66	303.2
Chitosan + 5% MMT	102.6	194.5	10.72	296.4
Chitosan + 1% 30B	103.1	193.1	6.33	299.2
Chitosan + 3% 30B	101.6	191.6	3.77	298.1
Chitosan + 5% 30B	102.9	188.5	3.62	298.6

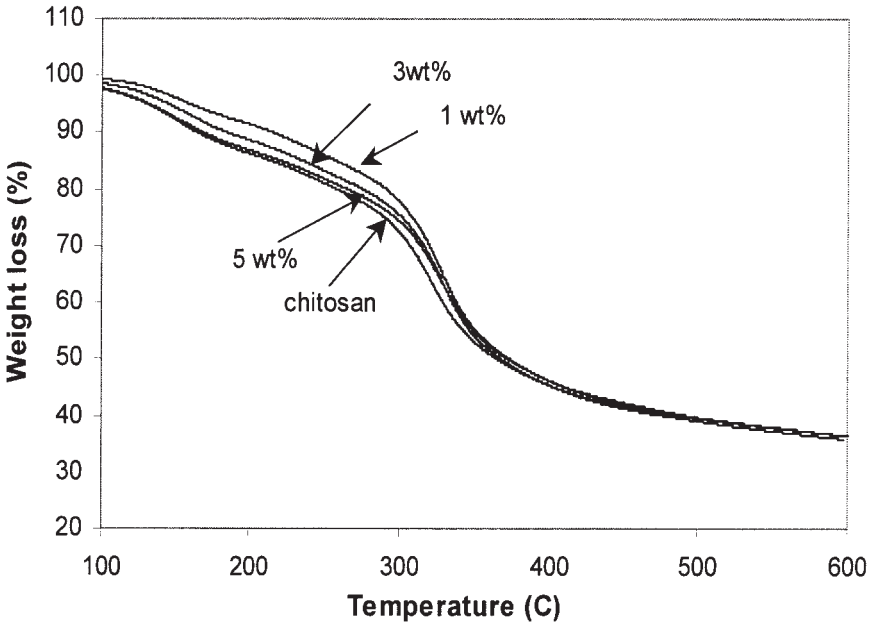

Figure 6 TGA curves of chitosan and its MMT-Na^+ nanocomposites with different MMT-Na^+ contents.

was added. T_m and T_d did not change significantly with addition of Cloisite 30B. Generally, addition of MMT-Na^+ improved the films mechanical and thermal properties more than Cloisite 30B.

The authors are grateful to Mr. Brian Jones in the Physics Department for use of the X- ray diffractometer, and to Dr. Kit Lee in the School of Biological Sciences for use of the TEM. This research was supported, in part, by funds provided through the Hatch Act.

References

1. Jung, B.; Kim, C. H.; Choi, K. S.; Lee, Y. M.; Kim, J. J. J Appl Polym Sci 1999, 72, 1719.
2. Boddu, V. M.; Smith, E. D. U.S. Pat. 20020043496 (2002).
3. Juang, R. S.; Shao, H. J. Water Res 2002, 36, 2999.
4. Klingels, M.; Griesbach, U.; Panzer, C.; Wachter, R. Henkel Referate 1999, 35, 78.
5. Mao, J. S.; Zhao, L. G.; Yao, K. D.; Shang, Q. X.; Yang, G. H.; Cao, Y. L. J Biomed Mater Res 2003, 64A, 301.
6. Risbud, M.; Hardikar, A.; Bhonde, R. J Biosci 2000, 25, 25.
7. Wu, J. J.; Zhu, T. Y.; Hu, L.; He, P.; Li, W. W. J China Burn 2002, 18, 19.
8. Kumar, S.; Jog, J. P.; Natarajan, U. J Appl Polym Sci 2003, 89, 1186.
9. Kim, J.-T.; Lee, D.-Y.; Oh, T.-S.; Lee, D.-H. J Appl Polym Sci 2003, 89, 2633.
10. Uyama, H.; Kuwabara, M.; Tsujimoto, T.; Nakano, M.; Usuki, A.; Kobayashi, S. Chem Mater 2003, 15, 2492.
11. McGlashan, S. A.; Halley, P. Polym Int 2003, 52, 1767.
12. Hay, J. N.; Shaw, S. J. Available at http://www.azom.com/details.asp?article ID=936 2000 (Accessed September 30, 2004).
13. Yamaguchi, I.; Tokuchi, K.; Fukuzaki, H.; Koyama, Y.; Takafuda, K.; Monma, H.; Tanaka, J. J Biomed Mater Res 2001, 55, 20.
14. ASTM. In Annual Book of ASTM Standards; American Society for Testing and Materials: West Conshohocken, PA, 1995; Vol. 8.01, p 182.
15. Di, Y. W.; Iannace, S.; Maio, E. D.; Nicolais, L. J Polym Sci Part B: Polym Phys 2003, 41, 670.
16. Choi, W. M.; Kim, T. W.; Park, O. O.; Chang, Y. K.; Lee, J. W. J Appl Polym Sci 2003, 90, 525.
17. Vaia, R. A.; Giannelis, E. P. Macromolecules 1997, 30, 8000.
18. Chen, X. C.; You, B.; Zhou, S. X.; Wu, L. M. Surf Interface Anal 2003, 35, 369.
19. Misra, M.; Park, H.; Mohanty, A. K.; Drzal, L. T. Paper Presented at the Global Plastics Environmental Conference, Detroit, MI, February 18, 2004.
20. Zheng, J. P.; Li, P.; Ma, Y. L.; Yao, K. D. J Appl Polym Sci 2002, 86, 1189.
21. Tortora, M.; Vittoria, V.; Galli, G.; Ritrovati, S.; Chiellini, E. Macromol Mater Eng 2002, 287, 243.
22. Priya, L.; Jog, J. P. J Appl Polym Sci 2003, 89, 2036.